Functional-Anatomic Fractionation of the Brain's Default Network

Jessica R. Andrews-Hanna, Jay S. Reidler, Jorge Sepulcre, Renee Poulin,
& Randy L. Buckner

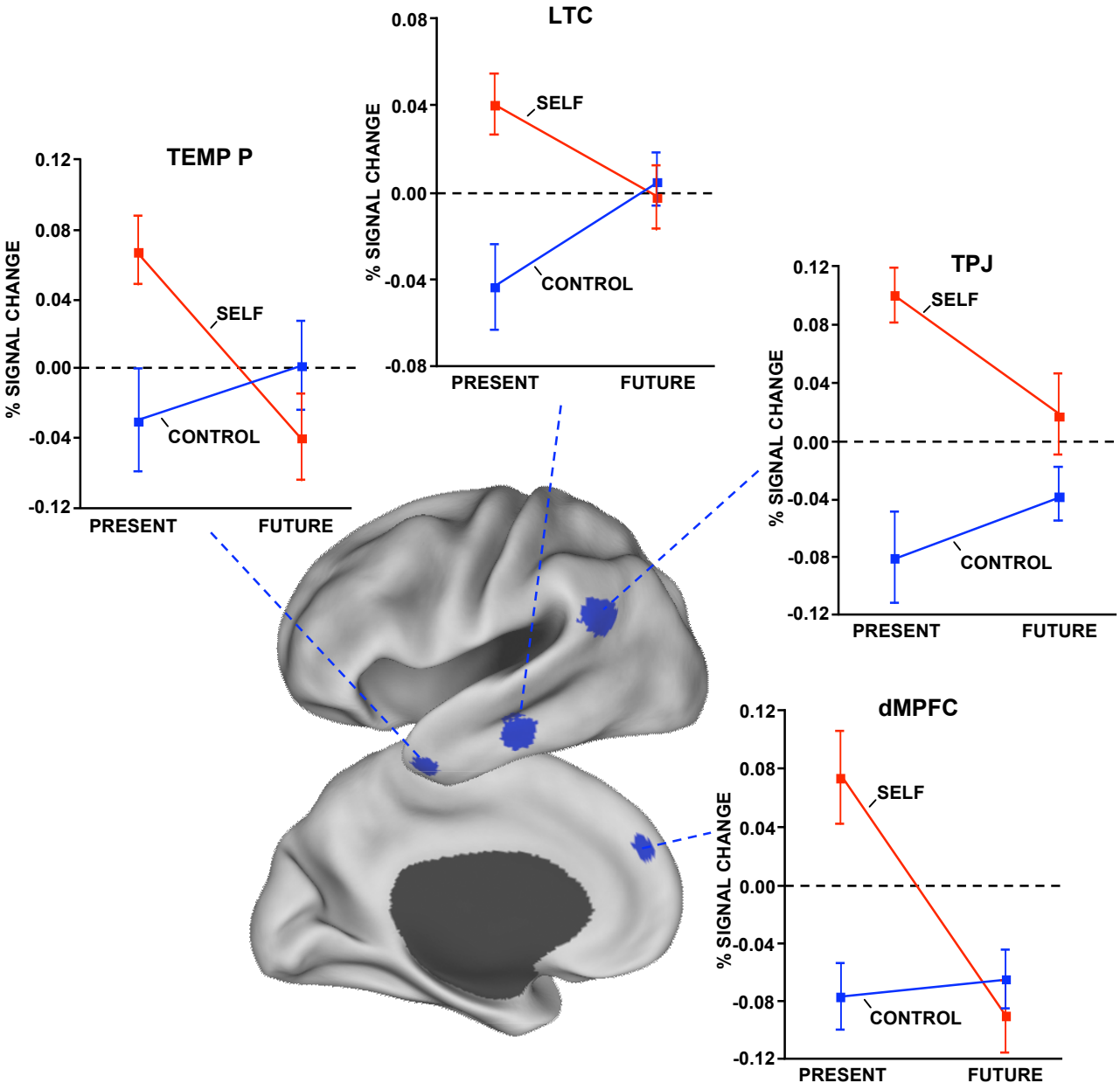

Figure S1: Regions within the dMPFC Subsystem Are Functionally-Coherent. Within each region comprising the dMPFC subsystem, the percent signal change is plotted for each of the four task conditions. Regions exhibit preferential activity for *Present Self* trials compared to *Future Self* trials, showing similar responses across regions. Note that since the activity magnitudes were controlled for RT, the zero value and +/- sign are relative. dMPFC = dorsal prefrontal cortex, TPJ = temporoparietal junction, LTC = lateral temporal cortex, TempP = temporal pole

Functional-Anatomic Fractionation of the Brain's Default Network

Jessica R. Andrews-Hanna, Jay S. Reidler, Jorge Sepulcre, Renee Poulin,
& Randy L. Buckner

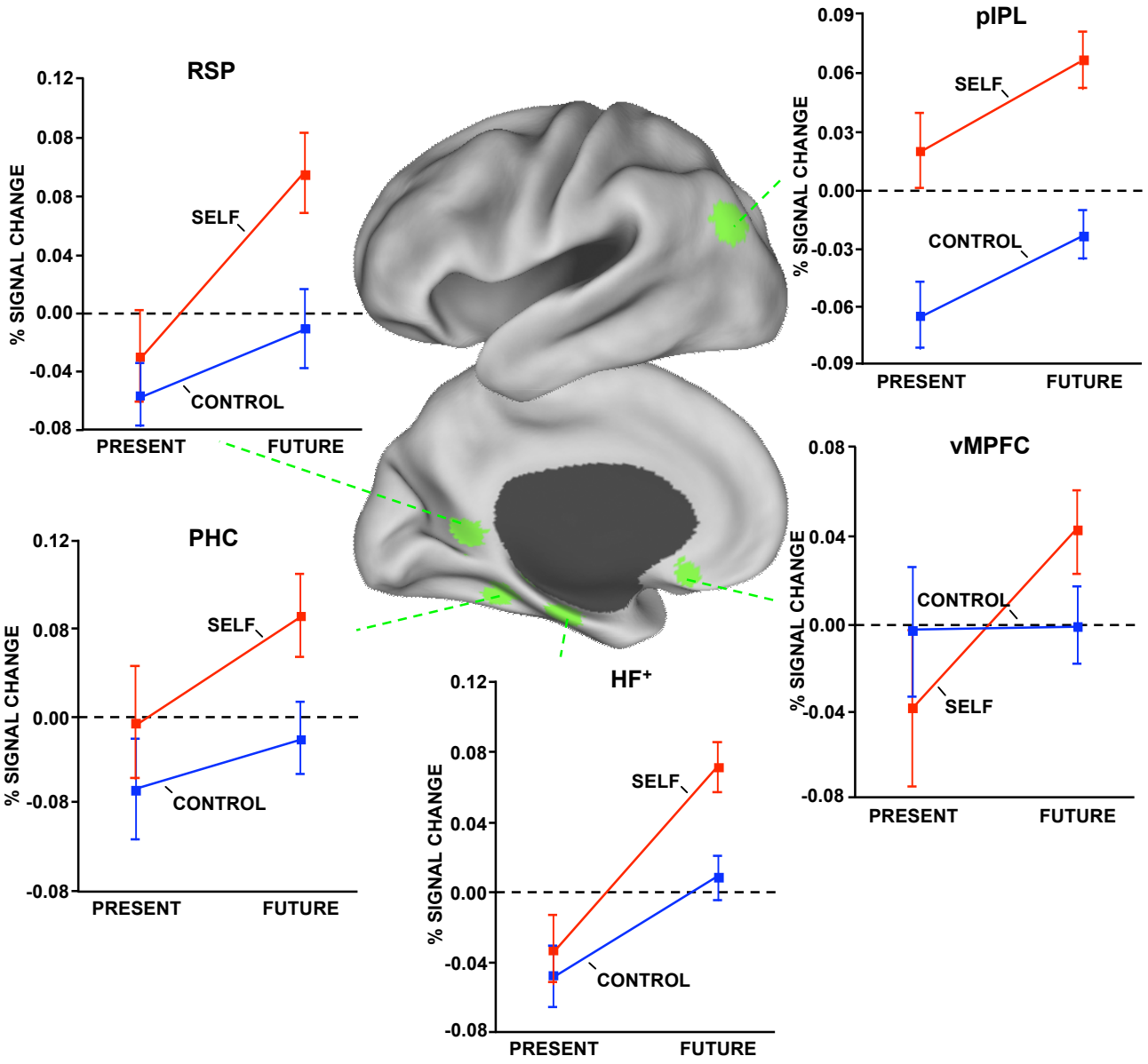

Figure S2: Regions within the MTL Subsystem Are Functionally-Coherent. Within each region comprising the MTL subsystem, the percent signal change is plotted for each of the four task conditions. Unlike the regions within the dMPFC subsystem, regions within the MTL subsystem exhibit preferential activity for *Future Self* trials compared to *Present Self* trials. Note that since the activity magnitudes were controlled for RT, the zero value and +/- sign are relative. vMPFC = ventral medial prefrontal cortex, pIPL = posterior inferior parietal lobule, Rsp = retrosplenial cortex, PHC = parahippocampal cortex, HF^{+} = hippocampal formation

Functional-Anatomic Fractionation of the Brain's Default Network

Jessica R. Andrews-Hanna, Jay S. Reidler, Jorge Sepulcre, Renee Poulin,
& Randy L. Buckner

Table S1: Regions of Interest

Region	Abbreviation	Broadman Areas	x	y	z
PCC-aMPFC Core					
Anterior medial prefrontal cortex	aMPFC	10,32	-6	52	-2
Posterior cingulate cortex	PCC	23,31	-8	-56	26
dMPFC Subsystem					
Dorsal medial prefrontal cortex	dMPFC	9,32	0	52	26
Temporal parietal junction	TPJ	40,39	-54	-54	28
Lateral temporal cortex	LTC	21,22	-60	-24	-18
Temporal pole	TempP	21	-50	14	-40
MTL Subsystem					
Ventral medial prefrontal cortex	vMPFC	11,24,25,32	0	26	-18
Posterior inferior parietal lobule	pIPL	39	-44	-74	32
Retrosplenial cortex	Rsp	29,30,19	-14	-52	8
Parahippocampal cortex	PHC	20,36,19	-28	-40	-12
Hippocampal formation	HF^{+}	20,36	-22	-20	-26

Note: Coordinates are based on the Montreal Neurological Institute coordinate system. Because regions are 8 mm spheres, Brodmann areas list approximate locations for reference.

Functional-Anatomic Fractionation of the Brain's Default Network

Jessica R. Andrews-Hanna, Jay S. Reidler, Jorge Sepulcre, Renee Poulin,
& Randy L. Buckner

Table S2: Statistical tests corresponding to Figure 2 of main text.

Default Network Component	Effect	$F(1,17)$	p
PCC-aMPFC Core	Self-Relevancy	17.70	< 0.005
	Orientation	0.56	0.47
	Self-Relevancy x Orientation	0.34	0.57
dMPFC Subsystem	Self-Relevancy	15.00	< 0.005
	Orientation	2.44	0.14
	Self-Relevancy x Orientation	27.00	< 0.001
MTL Subsystem	Self-Relevancy	7.82	< 0.05
	Orientation	17.20	< 0.005
	Self-Relevancy x Orientation	2.26	0.15

Note: dMPFC = dorsal medial prefrontal cortex; MTL = medial temporal lobe

Functional-Anatomic Fractionation of the Brain's Default Network

Jessica R. Andrews-Hanna, Jay S. Reidler, Jorge Sepulcre, Renee Poulin,
& Randy L. Buckner

Table S3. Strategy probes assessed in Experiment 3.

Strategy Probe Question	Present Self	Present Ctrl	Future Self	Future Ctrl
1. To what extent did this question ask about a matter that is significant to you?	**3.94 (1.06)**	2.54 (1.04)	**3.73 (0.61)**	2.89 (0.97)
2. To what extent did this question lead you to think about your own preferences, feelings or emotions?	**4.71 (1.30)**	2.71 (1.03)	**4.83 (0.46)**	2.87 (0.61)
3. To what extent did this question evoke any emotion (e.g. happiness, sadness, excitement, fear, etc.)?	**3.33 (0.77)**	2.49 (0.85)	**3.55 (0.73)**	2.70 (0.67)
4. How certain are you that your answer is (or will be) true?	**5.86 (0.42)**	4.14 (0.79)	**5.24 (0.57)**	4.00 (0.77)
5. To what extent did you rely on past experiences to answer this question?	3.93 (1.08)	4.05 (0.49)	**5.34 (0.60)**	4.36 (0.56)
6. To what extent did this question lead you to imagine events unfold in your mind?	2.75 (0.65)	2.71 (0.75)	**4.32 (0.43)**	3.45 (0.51)
7. To what extent did this question lead you to envision the location of the people, objects, or places mentioned in it?	3.99 (1.12)	4.30 (0.96)	**5.06 (0.54)**	4.05 (1.06)
8. To what extent did this question lead lead you to think about the future?	2.82 (1.01)	2.41 (1.03)	**4.68 (0.50)**	3.80 (0.85)
9. To what extent was this a factual, as opposed to a subjective, question?	3.34 (1.12)	**5.32 (1.03)**	3.92 (0.79)	**4.43 (0.93)**
10. To what extent did this question lead you to speculate about the preferences, emotions, or thoughts of other people?	2.55 (1.13)	**3.55 (1.45)**	2.67 (0.94)	**3.78 (1.02)**
11. How much did you have to think in order to answer this question?	2.40 (0.43)	**3.50 (0.36)**	2.79 (0.31)	**3.33 (0.41)**

Note: Values represent group mean. Standard deviation in parentheses.

Functional-Anatomic Fractionation of the Brain's Default Network

Jessica R. Andrews-Hanna, Jay S. Reidler, Jorge Sepulcre, Renee Poulin,
& Randy L. Buckner

Table S4: Participant Demographics.

Study	N	Age (mean)	Age range	# Male
Total*	**170**	**22.7**	**18-35**	**62**
Experiment 1 – MRI	**73**	**21.5**	**18-30**	**27**
Dataset 1 (ROI definition)	28	21.0	18-25	10
Dataset 2 (Clustering analysis)	45	21.8	18-30	17
Experiment 2 - MRI	**46**	**21.7**	**18-30**	**17**
Experiment 3 - Behavioral	**51**	**25.2**	**18-35**	**18**

Note: * = 41 participants completed both experiment 1 (dataset 2) and experiment 2 (MRI); therefore, n = 170 represents the number of data sessions (there were 129 independent participants).

Functional-Anatomic Fractionation of the Brain's Default Network

Jessica R. Andrews-Hanna, Jay S. Reidler, Jorge Sepulcre, Renee Poulin,
& Randy L. Buckner

SUPPLEMENTAL EXPERIMENTAL PROCEDURES

MRI data acquisition.

Magnetization prepared rapid acquisition gradient echo (MP-RAGE) 3D T1-weighted anatomical images were collected using the following sequence: repetition time (TR) = 2530 ms, echo time (TE) = 3.44 ms, inversion time (TI) = 1100 ms, flip angle = 7°, field of view (FOV) = 256 mm x 256 mm, matrix size = 256 x 256, 1 mm^3 voxel size, 256 slices. Functional data comprising Experiment 1 (dataset 2) and Experiment 2 were acquired with the following scanning parameters: TR = 2500 ms, TE = 30 ms, flip angle = 90°, FOV = 288 mm x 288 mm, matrix size = 96 x 96, 3 mm^3 voxel size, 3 mm slice thickness, 0.5 mm gap, 36 contiguous axial oblique slices aligned to the anterior commisure / posterior commisure plane, 156 separate interleaved acquisitions. Functional data comprising Experiment 1 (dataset 1) was acquired using slightly different parameters: TR = 3000 ms, TE = 30 ms, flip angle = 90, FOV = 288 mm x 288 mm, matrix size = 96 x 96, 3 mm^3 voxel size, 3 mm slice thickness, 0.5 mm gap, 43 contiguous axial oblique slices aligned to the anterior commisure / posterior commisure plane, 104 separate interleaved acquisitions.

Experiment 1: Analysis of default network architecture.

Functional connectivity preprocessing and analysis. The rest data comprising Experiment 1 has been contributed to the community as part of an open-source data release (http://www.nitrc.org/projects/fcon_1000/) and has been used for prior analyses within our own laboratory (Krienen and Buckner, 2009; Van Dijk et al., 2009). However, the analyses applied here are novel and not reported elsewhere. The three conditions (eyes open fixation, eyes open without fixation, eyes closed) were concatenated for all analyses. Recent studies have demonstrated topographically-similar connectivity within the default network across our included rest conditions (Yan et al., 2009; Van Dijk et al., 2009). It is for this reason that we pooled all of the available data to increase statistical power.

A number of preprocessing steps were performed on the data. The first four timepoints of each functional run were first removed to ensure stabilization of the BOLD

signal (FSL, FMRIB, Oxford, UK), followed by correction for differences in acquisition time between slices (SPM2, Wellcome Trust Center for Neuroimaging, London, UK). Next, a rigid-body correction for head motion within and across runs was performed (FSL, FMRIB, Oxford, UK). Nonlinear registration of functional data to a T2*-weighted Montreal Neurological Institute (MNI) template (SPM2, Wellcome Trust Center for Neuroimaging, London, UK) yielded images re-sampled at 2-mm cubic voxels.

Next, a series of functional connectivity-specific preprocessing techniques were performed extended from Biswal et al. (1995) and described in more detail in Van Dijk et al., 2009. Data within each session were first concatenated and spatially smoothed using a 6 mm full width half maximum (FWHM) kernel. Next, images were temporally filtered (low-pass) to retain frequencies below 0.08 Hz. A series of nuisance regressors reflecting spurious noise or systematic variance associated with non-neural sources was created and removed using partial regression. Nuisance regressors included the six parameters computed from the rigid-body motion correction, the averaged signal within a ventricular ROI, an ROI within the deep white matter, and an ROI comprising global gray matter. The first temporal derivative of each regressor was also included to account for temporal shifts in the BOLD signal. To create whole-brain correlation images, the averaged timeseries across all voxels comprising a seed ROI was used as the variable of interest in a linear regression with the timeseries corresponding to each voxel across the brain. In many cases, multiple ROIs were chosen and correlation coefficients between pairs of ROIs were computed by cross-correlating the averaged timeseries corresponding to each ROI. All statistical analyses of correlation data, including random-effects analyses, were performed on Fisher-z transforms (Zar, 1996), which unlike correlation coefficients, are approximately normally-distributed.

Network analysis. Pajek software (De Nooy et al., 2005) was used to build network graphs and to calculate betweenness-centrality measures. The Kamada-Kawai network analysis algorithm (Kamada and Kawai, 1989) employed in Pajek is described in more detail in the main text. Betweenness centrality for a given brain region, *a*, represents the proportion of all region-wise connections that pass through *a* and is expressed by the formula:

$$\sum_i \sum_j \frac{g_{iaj}}{g_{ij}} \quad \textit{where } i \neq j \neq a, \text{ and}$$

where g_{iaj} is the total number of geodesic paths (connections) between regions *i* and *j* that pass through *a,* while g_{ij} is the total number of paths connecting *i* and *j*. Thus, a region that exhibits high betweenness-centrality represents a candidate hub. Larger node circles were used to represent regions with high betweenness-centrality. Additional detail is available in a recent study that demonstrated the feasibility and reliability of these techniques in identifying cortical hubs (Buckner et al., 2009; see also Sporns et al., 2007, Hagmann et al., 2008).

Once we established that anterior medial prefrontal cortex (aMPFC) and posterior cingulate cortex (PCC) exhibited the highest betweenness measures and were correlated with every other region comprising the default network, our next question was to investigate the underlying functional-anatomic architecture of the remaining regions. Based on our preliminary investigations of intrinsic connectivity, combined with analysis of fMRI studies and anatomical connectivity in non-human primates (Buckner et al., 2008), we predicted that the hippocampal formation (HF+) would form a coherent cluster with the parahippocampal cortex (PHC), posterior inferior parietal lobule (pIPL), retrosplenial cortex (Rsp), ventral medial prefrontal cortex (vMPFC) and lateral parietal cortex (LTC). We also predicted the dorsal medial prefrontal cortex (dMPFC) would form a distinct cluster with temporparietal junction (TPJ) and temporal pole (TempP). Hierarchical clustering analysis allowed us to examine these predictions in an unbiased, quantative manner. For clustering analysis of subsystems, regions that exhibited the highest betweenness- centrality were classified as hubs and were subsequently omitted from analysis. Hierarchical clustering is a statistical algorithm frequently used in psychology and bioinformatics that partition s a set of variables (in this case, regions) into subsequently hierarchical clusters based on the "distances" or "similarities" between the variables (in this case, correlations between regions). Thus, regions that are strongly correlated with one another are likely to comprise the same cluster, and regions that are

weakly correlated are likely to comprise distinct clusters. Cluster graphs were viewed with Java TreeView (v1.1.3 http://jtreeview.sourceforge.net; Saldanha, 2004).

Experiment 2: Functional dissociation among default network subsystems.

Task paradigm. Four task conditions were included in the paradigm. *Future Self* questions asked about hypothetical autobiographical events that were to be experienced directly by the subject. The *Future Non-Self Control* questions asked parallel questions that required general semantic knowledge about the future and avoided reference to the participant. Temporal orientation was manipulated across conditions by either asking a question about the hypothetical event in the future or the immediate present. Across the *Self* and *Control* conditions, the clause within the sentence that oriented the subject to the timing of the event was counterbalanced. That is, if a question about the *Future Self* began by asking about an event "a few days from now" a separate *Future Non-Self Control* question would also use the same phrasing but not oriented to the self. Examples of questions are listed below:

Present Self*: Think about the major issues in your life at this moment. Which of these issues concerns you the most: health, education, or finance?*

Present Non-Self Control*: At this moment there is a leading candidate in the Republican Party for President. Which of the following candidates is that candidate: Mitt Romney, Senator John McCain, or Rudy Giuliani?*

Future Self*: Think about where you will be and who you will be with tomorrow afternoon during lunch. Who will you be eating lunch with: no one, your significant other, or someone else?*

Future Non-Self Control*: In two days, a sporting event will be televised by reporters in the southwest United States. Is the type of sport more likely to be: rodeo, baseball, or another type of sport?*

Functional-Anatomic Fractionation of the Brain's Default Network

Jessica R. Andrews-Hanna, Jay S. Reidler, Jorge Sepulcre, Renee Poulin,
& Randy L. Buckner

Data processing and statistical analyses. A number of preprocessing and analysis steps were implemented using SPM2 software (Wellcome Trust Center for Neuroimaging, London, UK). These procedures included discarding the first four timepoints of each functional run to allow for scanner equilibrium effects, correcting for differences in slice acquisition time and motion between volumes, nonlinear atlas registration to a T2*-weighted MNI template (re-sampled at 2-mm cubic voxels), and spatial smoothing using a 6 mm FWHM kernel. SPM2 (Wellcome Trust Center for Neuroimaging, London, UK) was also used to construct and implement the general linear model for fMRI statistical analysis. For each of four conditions, a canonical hemodynamic response function along with its temporal derivative was convolved with a 10 s boxcar function at the onset of each trial. Separate run regressors were modeled to control for mean differences between runs and a regressor reflecting the mean of all four runs was also included in the model. Data were temporally filtered (high-pass using a cutoff of 128 s) to remove scanner drift and other sources of variance thought to be unrelated to the tasks. Hypothesis-driven analyses involved extracting the magnitude of activity in the *a priori* ROIs created in Experiment 1 using in-house software. Exploratory, whole-brain group analyses involved subjecting each participant's fixed-effects condition contrasts to random-effects analyses, thresholded at $p < 0.0001$ uncorrected.

Functional-Anatomic Fractionation of the Brain's Default Network

Jessica R. Andrews-Hanna, Jay S. Reidler, Jorge Sepulcre, Renee Poulin,
& Randy L. Buckner

SUPPLEMENTAL REFERENCES

Biswal, B., Yetkin, F.Z., Haughton, V.M., and Hyde, J.S. (1995). Functional connectivity in the motor cortex of resting human brain using echo-planar MRI. Magn. Res. Med. *34*, 537-41.

Buckner, R.L., Sepulcre, J., Talukdar, T., Krienen, F.M., Liu, H., Hedden, T., Andrews-Hanna, J.R., Sperling, R.A. and Johnson, K.A. (2009). Cortical hubs revealed by intrinsic functional connectivity: mapping, assessment of stability, and relation to Alzheimer's disease. J. Neurosci. *29*, 1860-1873.

Buckner, R.L., Andrews-Hanna, J.R., and Schacter, D.L. (2008). The brain's default network: anatomy, function and relevance to disease. Ann. N.Y. Acad. of Sci. *1124*, 1-38.

De Nooy, W., Mrvar, A., and Batageli, V. (2005). Exploratory network analysis with Pajek (New York, Cambridge).

Hagmann, P., Cammoun, L., Gigandet, X., Meuli, R., Honey, C.J., Wedeen, V.J., and Sporns, O. (2008). Mapping the structural core of human cerebral cortex. PLoS Biol. *6*, e159.

Kamada, K., and Kawai, S. (1989). An algorithm for drawing general undirected graphs. Information Process Letters *31*, 7-15.

Krienen, F.M., and Buckner, R.L. (2009). Segregated fronto-cerebellar circuits revealed by intrinsic functional connectivity. Cereb. Cortex *19*, 2485-2497.

Saldanha, A.J. (2004). Java Treeview – extensible visualization of microarray data. Bioinformatics *20*, 3246-3248.

Sporns, O., Honey, C.J., and Kotter, R. (2007). Identification and classification of hubs in brain networks. PLoS ONE *2*, e1049.

Van Dijk, K.R., Hedden, T., Venkataraman, A., Evans, K.C., Lazar, S.W., and Buckner, R.L. (2009). Intrinsic functional connectivity as a tool for human connectomics: theory, properties, and optimization. J. Neurophysiol. Doi:10.1152/jn.00783.2009.

Yan, C., Liu, D., He, Y., Zou, Q., Zhu, C., Zuo, X, Long, X., and Zang, Y. (2009). Spontaneous brain activity in the default mode network is sensitive to different resting-state conditions with limited cognitive load. PLoS ONE *4*, e5743.

Zar, J.H. (1996). Biostatistical Analysis (Upper Saddle River: Prentice-Hall).